Article

Discovery and Optimization of a Synthetic Class of Nectin-4-Targeted CD137 Agonists for Immuno-oncology

Punit Upadhyaya, Julia Kristensson, Johanna Lahdenranta, Elizabeth Repash, Jun Ma, Jessica Kublin, Gemma E. Mudd, Lia Luus, Phil Jeffrey, Kristen Hurov, Kevin McDonnell, and Nicholas Keen*

ABSTRACT: CD137 (4-1BB) is a co-stimulatory receptor on immune cells and Nectin-4 is a cell adhesion molecule that is overexpressed in multiple tumor types. Using a series of poly(ethylene glycol) (PEG)-based linkers, synthetic bicyclic peptides targeting CD137 were conjugated to *Bicycles* targeting Nectin-4. The resulting bispecific molecules were potent CD137 agonists that require the presence of both Nectin-4-expressing tumor cells and CD137-expressing immune cells for activity. A multipronged approach was taken to optimize these *Bicycle* tumor-targeted immune cell agonists by exploring the impact of chemical configuration, binding affinity, and pharmacokinetics on CD137 agonism and antitumor activity. This effort resulted in the discovery of BT7480, which elicited robust CD137 agonism and maximum antitumor activity in syngeneic mouse models. A tumor-targeted approach to CD137 agonism using low-molecular-weight, short-acting molecules with high tumor penetration is a yet unexplored path in the clinic, where emerging data suggest that persistent target engagement, characteristic of biologics, may lead to suboptimal immune response.
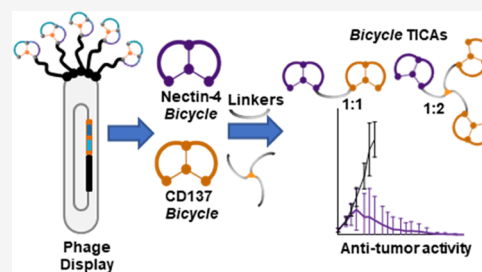
INTRODUCTION

Checkpoint inhibitor antibodies have revolutionized immunotherapy in cancer, however, first-generation immune co-stimulatory receptor agonist antibodies have shown limited success in the clinic.[1−3] CD137 (4-1BB) is an important co-stimulatory receptor expressed on activated CD8+ T cells, activated CD4+ helper T cells, B cells, regulatory T cells, natural killer cells, and natural killer T cells.[4,5] The anti-CD137 monoclonal antibody agonist urelumab has demonstrated efficacy in clinical trials but clinical utility was limited by on-target hepatotoxicity.[2] A new generation of monoclonal antibodies (mAbs), antigen-binding fragments (Fabs), designed ankyrin repeat proteins (DARPins), and other modalities that address the challenges of the first-generation CD137 agonist molecules are now under evaluation in the clinic.[6−11] While these molecules have shown promising preclinical results, as recombinant protein modalities, they still share common limitations with their predecessors that may eventually limit their clinical utility, including poor penetration into solid tumors, long-circulating terminal half-lives, and high potential for immunogenicity.[12,13]

Macrocyclic peptides discovered using different de novo screening/selection technologies have recently graduated from molecules with interesting biology, limited by nondrug-like properties, to bona fide clinical assets addressing unmet medical needs in numerous therapeutic areas.[14−16] Bicyclic peptides, or *Bicycles*, are a class of highly constrained peptides characterized by the formation of two loops when the linear peptide is cyclized around a trivalent scaffold. *Bicycles* are currently being explored

in the clinic as an inhibitor of kallikrein for ocular indications and *Bicycle* toxin conjugates (BTCs) for targeted delivery of cytotoxic payloads into tumors.[17,18]

We sought to expand the utility of *Bicycles* as differentiated tumor-targeted and tumor antigen-dependent CD137 agonists. We hypothesized that these molecules may offer two advantages over other modalities: (1) their small size (4−10 kDa) compared to large recombinant biological molecules such as mAbs (150 kDa) results in high tumor penetrance and may afford a more native-like immune synapse when a tumor antigen is employed as a surrogate for CD137L and (2) a short systemic exposure may prevent T-cell exhaustion/activation-induced cell death of lymphocytes. In contrast to checkpoint inhibition, where complete saturation of the receptors drives the reversal of immunosuppression, intermittent target engagement that reflects the physiological context of T-cell co-stimulation may be more appropriate for a CD137 agonist.[19,20]

The first series of these *Bicycle* tumor-targeted immune cell agonists (*Bicycle* TICAs) was recently reported, and the generalizability and modularity of the approach along with the application of *Bicycle* TICAs targeting EphA2 to treat tumors preclinically were described.[21] We have also progressed a second
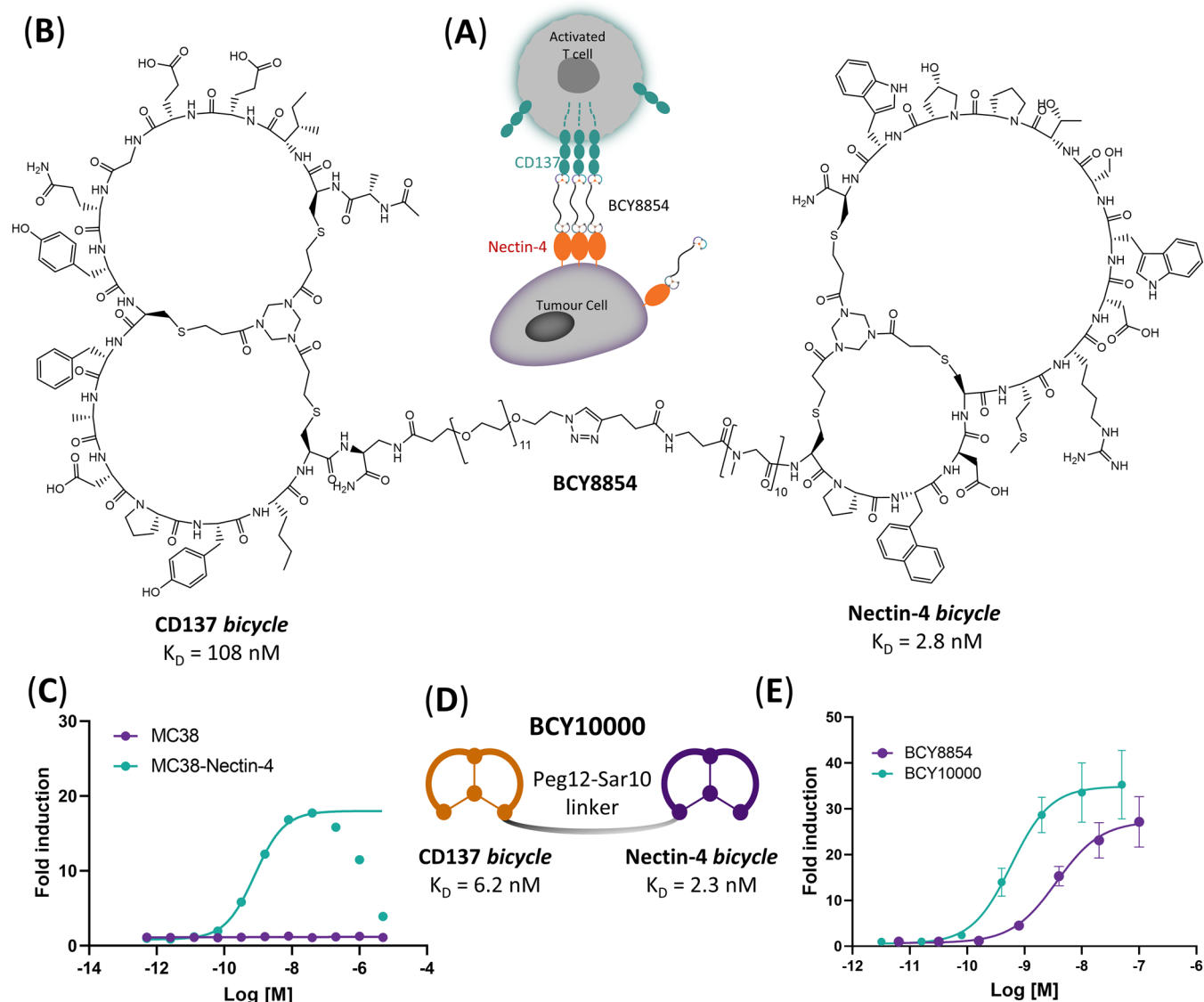
Figure 1. First Nectin-4/CD137 *Bicycle* TICA demonstrates Nectin-4-dependent CD137 agonism. (A) Schematic illustration of Nectin-4-dependent CD137 agonism induced by BCY8854. (B) Structure of BCY8854 with a linker composed of Peg12 and Sar10 and affinities to CD137 and Nectin-4 as measured by SPR. (C) CD137 reporter coculture assay activity with MC38 (Nectin-4 negative) or MC38-Nectin-4 tumor cells after treatment for 6 h with BCY8854. Data are mean ($n = 2$ replicates). (D) Pictorial representation of BCY10000, where Nectin-4 bicycle, linker, and attachment point are the same as BCY8854, but the CD137 bicycle is replaced with higher affinity analogue. The binding affinities (K_D) to CD137 and Nectin-4 as measured by SPR are also shown. (E) HT1376/CD137 reporter coculture assay activity of BCY8854 and BCY10000. Data are mean $\pm$ s.d ($n = 3$ replicates) and represented as fold induction over the background of a luciferase reporter gene driven by an element that responds to CD137 stimulation. Data in panels (C) and (E) were fit using log (agonist) vs response—variable slope (four parameters) in GraphPad Prism V.8.4.3.

program targeting Nectin-4-expressing tumors. Nectin-4 is highly expressed in a wide range of solid tumors, including bladder cancer, breast cancer, including triple-negative breast cancer, gastric/upper gastrointestinal (GI) cancer, non-small cell lung cancer, ovarian cancer, melanoma, and pancreatic cancer.[22,23]

Here, we describe the genesis of BCY11863 (BT7480), starting from the first *Bicycle* TICA synthesized to the clinical candidate and present a retrospective analysis of the effects of different variables on potency and efficacy. A medicinal chemistry approach to optimizing this type of dual tumor/ immune cell targeting moiety is unprecedented in the literature because this is the first example of a class of fully synthetic and <10 kDa MW ligands that can co-ligate a target antigen on tumor cells and a co-stimulatory receptor on immune cells.

Through this medicinal chemistry campaign, the roles of linker length, affinity, stoichiometry, hinge composition, pharmacokinetics, and target expression were elucidated to develop the first-in-class clinical candidate *Bicycle* TICA. The pharmacology of BT7480 has recently been described and it is currently undergoing clinical trial (ClinicalTrials.gov Identifier: NCT05163041).[24]

RESULTS

In Vitro Proof of Concept. To (a) explore the possibility of directing CD137 agonism to Nectin-4-expressing tumors and (b) assess the potential of tumor antigen Nectin-4 to provide a scaffolding function to oligomerize and present a CD137 *Bicycle* to immune cells in a manner that leads to tumor antigen-dependent activation (Figure 1A), a previously identified
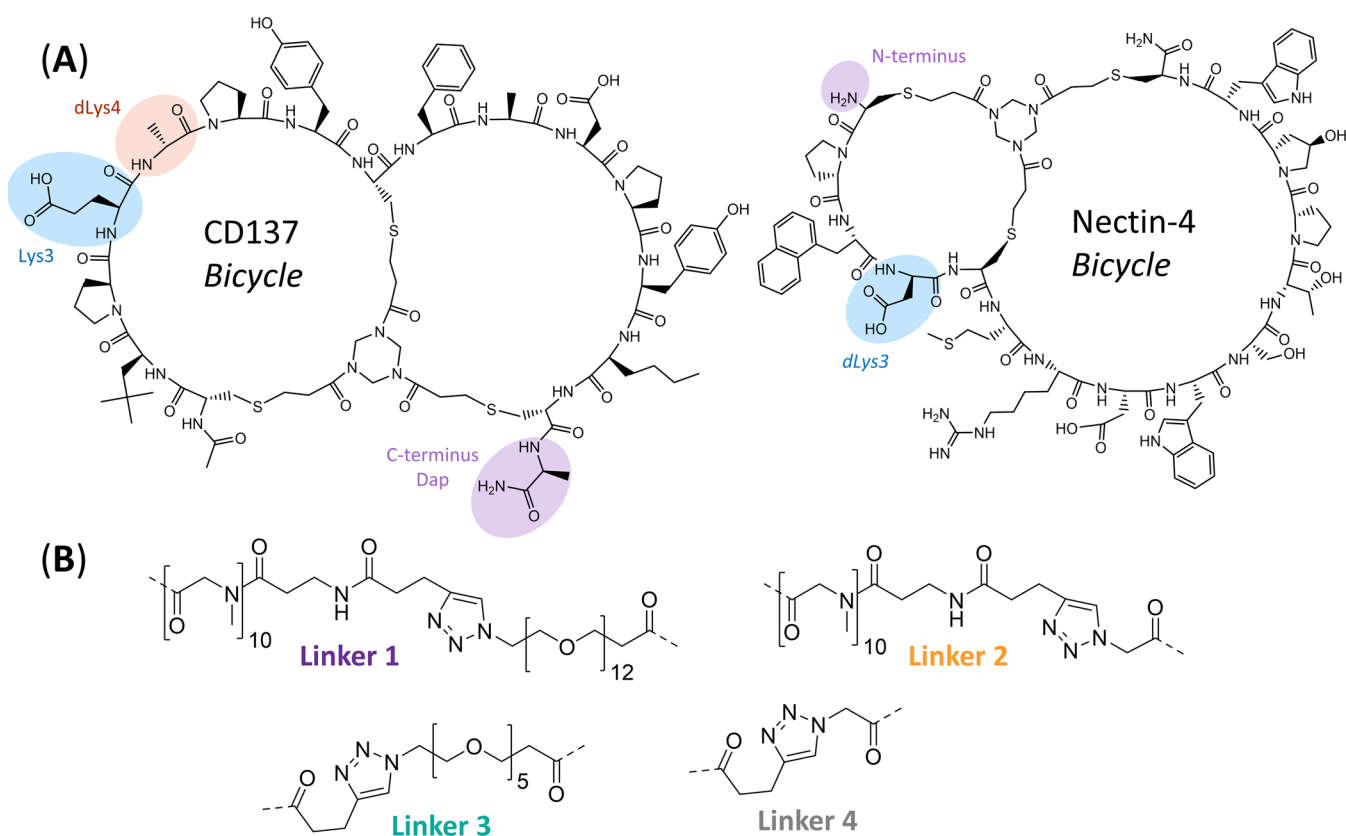
Figure 2. Chemical structures of representative CD137 and Nectin-4 *Bicycles* and linkers used in the synthesis of *Bicycle* TICAs. (A) Structure of CD137-binding bicycle (left). One of the three positions highlighted was modified to incorporate nucleophilic amine containing amino acids (Lys3, dLys4, C-terminal Dap). Nectin-4-binding *Bicycle* (right) with N-terminal amine or dAsp3 → dLys3 substitution used for conjugation highlighted. (B) Structure of four linkers used to assess the impact of linker length on the potency of *Bicycle* TICAs. Dashed bonds represent the attachment point to Nectin-4- or CD137-binding *Bicycle* via an amide bond.

Nectin-4-targeting *Bicycle* was adopted as a starting point. The initial design involved directly conjugating this chemically optimized Nectin-4-binding bicyclic peptide together with its 10-sarcosine linker with an additional PEG12 linker to a CD137-binding *Bicycle*, resulting in BCY8854 (Figure 1B). BCY8854 retained binding to both receptors with individual affinities to Nectin-4 and CD137 determined by surface plasmon resonance (SPR) to be $K_D = 2.8$ and 108 nM, respectively (Table S1). When this simple prototype bispecific compound was added to a coculture system containing a murine colon adenocarcinoma cell line engineered to express Nectin-4 (MC38-Nectin-4) or the corresponding parental line that does not endogenously express Nectin-4 (MC38) and a CD137-overexpressing Jurkat reporter cell line (hereby, referred to as the tumor cell/CD137 reporter coculture assay), dose-dependent agonism of CD137 was observed only in the presence of the Nectin-4-expressing MC38 clone (Figure 1C). As anticipated for a bispecific molecule that forms ternary complexes, BCY8854 showed reduced agonism at concentrations above 300 nM. This is referred to as a "hook effect" and is anticipated to be seen at concentrations, where one or both targets become limiting.[25] CD137 agonism was also observed with BCY8854 in coculture with human tumor cell lines HT1376 and NCI-H292 that endogenously express Nectin-4 and a CD137-overexpressing Jurkat reporter cell line but not with a Nectin-4 null PC3 cell line.[21]

A parallel medicinal chemistry effort undertaken (manuscript in preparation) to optimize the potency of the CD137-binding

Bicycle led to the discovery of BCY7965 with an improved affinity of 4 nM as measured by SPR (Table S1). Incorporation of this higher affinity CD137 binder in BCY10000 improved the in vitro potency (EC50) by fourfold and E_{max} by 1.5 fold in the HT1376/CD137 reporter coculture assay (Figure 1D,E). BCY8854 and BCY10000 demonstrated the proof of concept for a Nectin-4-dependent *Bicycle* TICA approach and served as the starting point for further medicinal chemistry optimization efforts.

Exploring Affinity, Linker Length, and Attachment Point. Due to the modular nature of the *Bicycles*, several analogues of BCY8854 and BCY10000 were synthesized to explore the effects of affinity, linker length, and attachment point of the *Bicycles* on the potency. Three attachment points on the CD137 *Bicycle* were explored, where one of the amino acid side chains was replaced with primary amine groups for conjugation: C-terminal Ala → Dap, Glu3 → Lys3, and dAla4 → dLys4. Similarly, two attachment points for conjugation to the Nectin-4 *Bicycle* were explored: N-terminal amine and dAsp3 → dLys3 substitution (Figure 2A and Table S7). These attachment points did not significantly impact binding to their respective targets, i.e., substitution of these positions with alternate amino acids had little to no impact on affinity (data not shown). The linkers evaluated spanned a range of lengths from 79 atoms (linker 1) to 8 atoms (linker 4) (Figure 2B). Ten *Bicycle* TICAs (synthesis and full structure in the Supporting Information) were assessed in the HT1376/CD137 reporter coculture assay using BCY10000 as the plate control. Remarkably, changing the
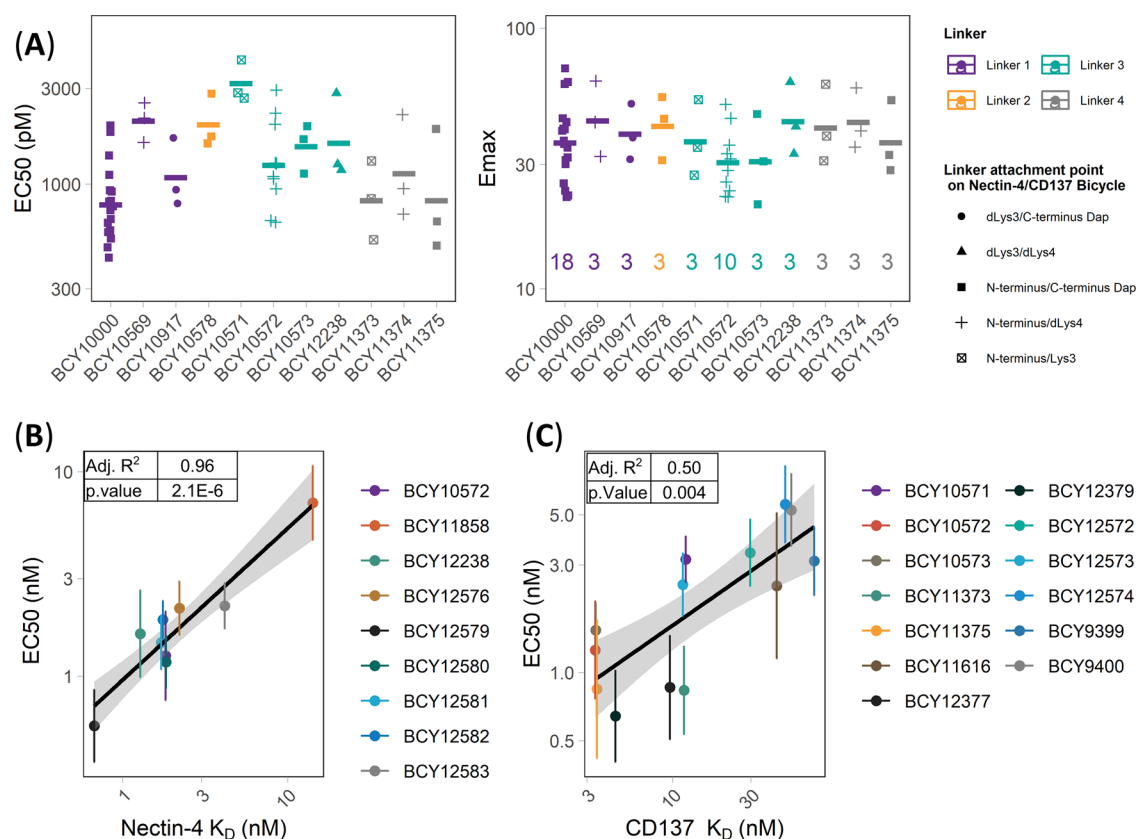
Figure 3. Exploring the structure−activity relationship of 1:1 Nectin-4/CD137 *Bicycle* TICA. (A) Nectin-4/CD137 *Bicycle* TICAs containing the same CD137 and Nectin-4 binders, but different linker lengths and attachment point (structures in Figure 2) were assessed in the HT1376/CD137 reporter coculture assay. Individual EC50 and E_{max} (fold induction over background) were reported as points, geometric means as crossbars, and the number of replicates (n) shown on the E_{max} plot. Colors represent the linkers and shapes represent the attachment points on the Nectin-4/CD137 *Bicycles* (B, C) EC50 (nM) determined in HT1376/CD137 reporter coculture assay of *Bicycle* TICAs that have the (B) same CD137 *Bicycles* (BCY8928) but different Nectin-4 *Bicycles* or (C) same Nectin-4 *Bicycle* (BCY8116) but different CD137 *Bicycles* plotted against binding affinities (K_D) to (B) Nectin-4 and (C) CD137 as measured by SPR. EC50 was reported from at least three independent experiments. SPR (K_D) was measured using at least four concentrations of *Bicycle* TICA to obtain k_{on}, k_{off}, and K_D. Adjusted R^2 and p value are reported from the linear regression model of mean EC50 (nM) vs K_D (nM).

linker length (Figure 2B) and attachment point (Figure 2A) led to no significant changes in activity (EC50 and E_{max}) indicating a high degree of flexibility of the binding mode of the bispecific molecules (Figure 3A and Table S2). For example, BCY10572 which contains a Nectin-4 *Bicycle* (BCY8116, Table S7) conjugated via the N-terminus (Figure 2A) to a PEG5 linker (linker 3, Figure 2B) via an amide bond and a CD137 *Bicycle* (BCY8928, Table S7) via click chemistry has a similar EC50 and E_{max} in the HT1376/CD137 coculture reporter assay to BCY11374, which has the same Nectin-4 and CD137 *Bicycles* as BCY10572 but contains a much shorter linker (linker 4, Figure 2B). One exception to the lack of differences in potency in the series was BCY10571. BCY10571 has a PEG5 linker (linker 3, Figure 2B) and Lys3 attachment on the CD137 *Bicycle*, which exhibited an EC50 two- to threefold weaker than similar compounds with either dLys4 (BCY10572) or C-terminal Dap (BCY10573) attachment.

The impact of the *Bicycle* TICA binding affinity to both targets on CD137 agonism was evaluated. Two sets of *Bicycle* TICAs were selected for analysis: (a) compounds with the same CD137 *Bicycle* (BCY8928), but different Nectin-4 *Bicycles* (Nectin-4 K_D range (20-fold): 0.7−14 nM), and (b) compounds with the same Nectin-4 *Bicycle* (BCY8116), but different CD137 *Bicycles* (CD137 K_D range (20-fold): 3.4−73 nM) (see CSV file in the Supporting Information). Evaluation of this series in the

HT1376/CD137 reporter coculture assay system and SPR binding experiments to both Nectin-4 and CD137 (Figure 3B,C) demonstrated that the potency of the *Bicycle* TICA is correlated to the binding affinity for both monomers (p-value of 2.1×10^{-6} and 0.004, respectively). However, the EC50 was much more sensitive to the affinity to Nectin-4 (adjusted R^2 = 0.96) than to CD137 (adjusted R^2 = 0.50). Indeed, improving the CD137 affinity from 73 nM (BCY9399) to 3.5 nM (BCY11375) only improved the EC50 by 3.6-fold while improving the Nectin-4 affinity from 14 nM (BCY11858) to 0.67 nM (BCY12579) resulted in improvement of EC50 by 12-fold (Tables S1 and S2). This indicates that the binding affinity of the tumor-targeting *Bicycle* had a more substantial impact on potency than modulating the immune cell engaging arm.

Exploring Valency. CD137 on immune cells is activated by engagement with its native ligand CD137L, a homotrimeric protein found on antigen-presenting cells.[26] Agonistic CD137 antibodies achieve different degrees of receptor activation via antibody-mediated dimerization and through higher-order clustering by Fc receptors.[27] To explore the impact of valency of both the Nectin-4- and CD137-binding arms on the activity of the *Bicycle* TICAs, a series of hinges with different valencies were synthesized (Figure 4A) and the ratios of Nectin-4 and CD137 binders were controlled using orthogonal or sequential conjugation steps (Supporting Information). Significant im-
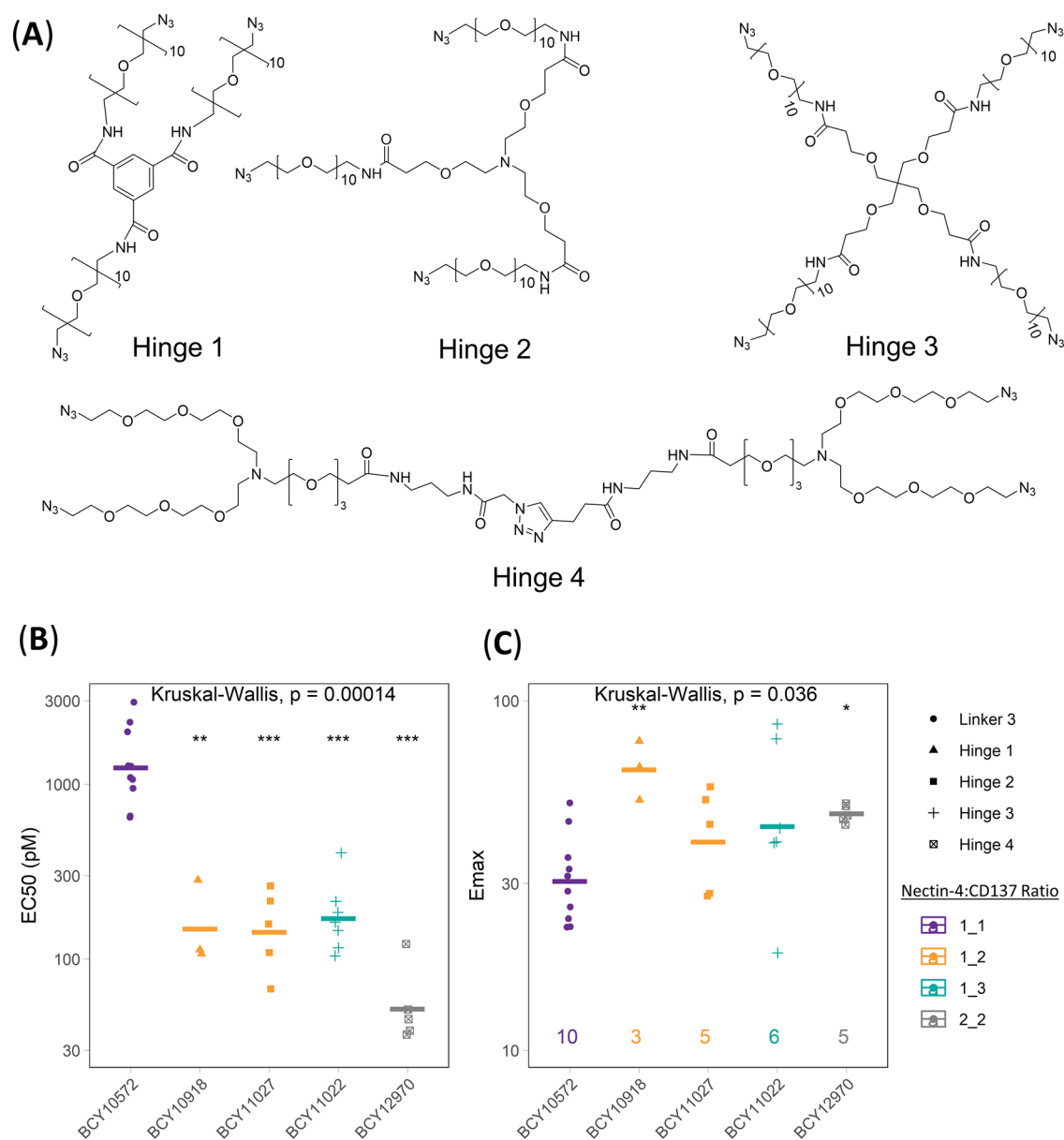
Figure 4. Exploring the structure−activity relationship of Nectin-4/CD137 *Bicycle* TICAs by modulating the ratio of CD137 and Nectin-4 *Bicycles*. (A) Structure of four hinges used to assemble different ratios of Nectin-4/CD137 *Bicycles* into *Bicycle* TICAs. (B) EC50 and (C) E_{max} (fold induction over background) of *Bicycle* TICAs determined in HT1376/CD137 reporter coculture assay. Individual data from each experiment shown as points, geometric mean as crossbars, and number of replicates on the bottom of E_{max} plot. Shapes represent hinge or linker, and color represents valency of Nectin-4/CD137 *Bicycles* in the *Bicycle* TICA. The global test for significance was performed using a Kruskal−Wallis nonparametric test. Multiple pairwise tests with BCY10572 as a reference group were performed using the Mann−Whitney U test.

provements in both EC50 (8.3-fold) and E_{max} (2.0-fold) were observed in the HT1376/CD137 reporter coculture assay when the ratio of Nectin-4/CD137 was changed from 1:1 (BCY10572) to 1:2 (BCY10918) using a trimesic acid/ PEG10 based 3-armed hinge (hinge 1, Figure 4) with similar improvements seen with the 1:2 molecule (BCY11027) synthesized using hinge 2. There were no significant improvements in EC50 or E_{max} by increasing the valency further from 1:2 to 1:3, which was synthesized using hinge 3 (Figure 4A). Additionally, and as previously described, homotrimers of CD137 *Bicycles* can achieve potent agonism of CD137 independent of tumor antigen binding.[21] As the design goal for the *Bicycle* TICA was complete dependence on tumor targeting for activity, a 1:3 molecule, such as BCY11022, that

could potentially be active in nontumor tissues was not pursued further. The 2:2 molecule BCY12970 synthesized using hinge 4 was 2.9-fold more potent than the 1:2 format with a similar E_{max} (Figure 4). While this was a modest improvement, it was not substantial enough to warrant the potentially more complex manufacturing steps that would come in later stages of development. A 2:1 Nectin-4/CD137 (BCY11384) valency synthesized using hinge 2 was also considered, but the E_{max} was lower with no improvement in EC50 compared to 1:1 format (Table S2). The 1:2 Nectin-4/CD137 valency was therefore selected as the lead format for further medicinal chemistry optimization.

Exploring the Structure−Activity Relationships of 1:2 *Bicycle* TICAs. A commercially available 1:2 hinge (hinge 5,
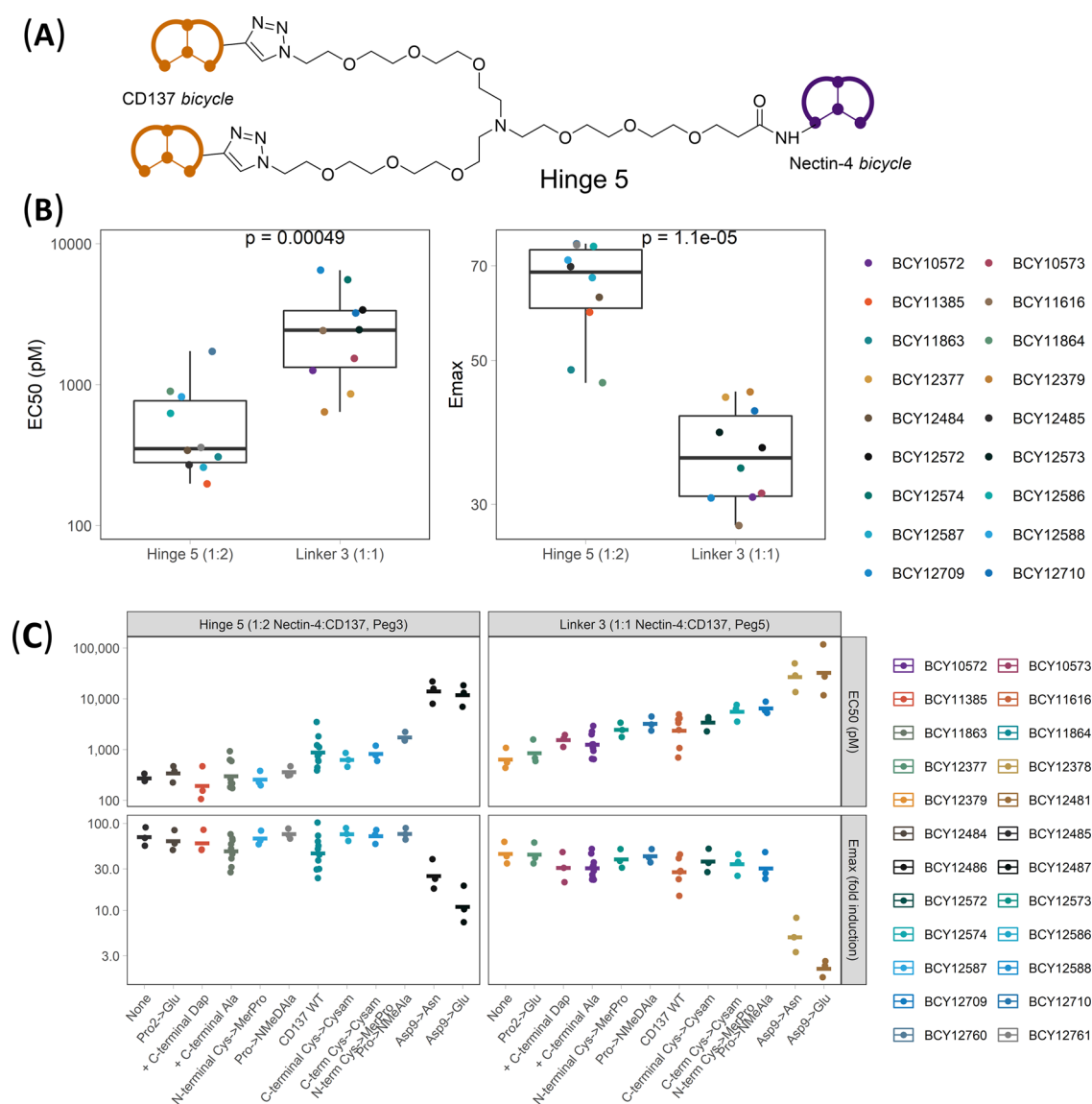
Figure 5. Exploring the structure−activity relationship of Nectin-4/CD137 *Bicycle* TICAs by introducing point mutations to CD137-binding *Bicycle*. (A) Structure of hinge 5. (B) Box and whisker plot of the geometric mean of EC50 and E_{max} of each *Bicycle* TICA (excluding substitution Asp9 → Asn and Asp9 → Glu that substantially impacted binding affinity) synthesized in the 1:1 format using linker 3 and 1:2 format using hinge 5 in the determined in HT1376/CD137 reporter coculture assay. The test for significance was performed using the Mann−Whitney U test. (C) EC50 and E_{max} of *Bicycle* TICAs from the HT1376/CD137 reporter coculture assay shown as individual data points with geometric mean represented as crossbars. The *x*-axis represents point mutations to the CD137 *Bicycle* of the *Bicycle* TICA as compared to BCY12379 (linker 3, 1:1) and BCY12485 (hinge 5, 1:2).

Figure 5A) was adopted to improve the synthetic tractability of the 1:2 *Bicycle* TICAs. Using this hinge, a series of molecules were created that explored the effect of modifications to the CD137 and Nectin-4 binders on the potency, solubility, and pharmacokinetics of the 1:2 *Bicycle* TICAs. This series of molecules was compared to 1:1 Nectin-4/CD137 *Bicycle* TICAs that had the same set of Nectin-4- and CD137-binding *Bicycles* in the HT1376/CD137 coculture reporter assay. The 1:2 format had 4.8-fold lower EC50 compared to the 1:1 format (geometric mean EC50 = 0.46 vs 2.2 nM) and 1.8-fold higher E_{max} (geometric mean E_{max} = 64 vs 36 fold induction over background) (Figure 5B). When compared like for like according to substitutions of amino acids within the CD137-binding arm of the molecule, the trend for potency is similar (Figure 5C). A detailed analysis of the structure−activity relationship based on substitutions to the CD137 *Bicycle* and its

impact on binding affinity in the context of the cocrystal structure is described elsewhere (manuscript under preparation). Interestingly, substitutions that significantly weakened the binding affinity to CD137 (Asp9 → Glu, Asn) substantially reduced the activity in the 1:1 format, but when incorporated into the 1:2 format, the impact on EC50 (14 and 12 nM, respectively) and E_{max} (25- and 11-fold induction over background, respectively) was less severe. Having two CD137 binders may induce higher-order clustering or provide enhanced affinity through avidity effects, and this may explain the greater retained activity for the 1:2 format. Consistent with this hypothesis, it was demonstrated by SPR that 1:2 molecules BCY12486 and BCY12487 bound to immobilized CD137 with an apparent K_D of around ∼8 nM, whereas the 1:1 analogues (BCY12378 and BCY12481) bind with K_D of 878 and 2.37 μM, respectively (Figure S1).
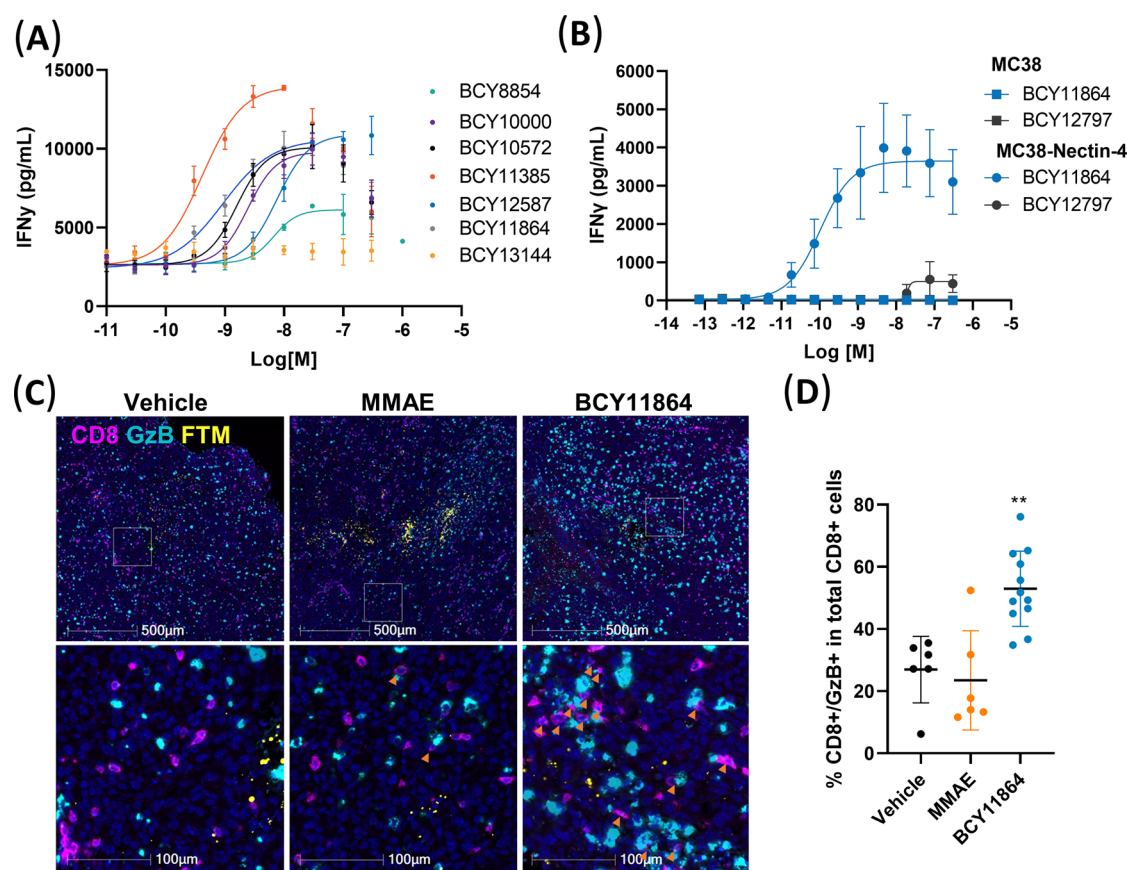
Figure 6. In vitro functional activity and in vivo pharmacodynamics of Nectin-4/CD137 *Bicycle* TICA. (A) Human PBMCs cocultured with HT1376 cell line were treated with anti-CD3 (OKT3) to induce CD137 expression and *Bicycle* TICAs were added. (B) Human PBMCs cocultured with mouse MC38 cell line or MC38-Nectin-4 were treated with anti-CD3 (OKT3) and BCY11864 or BCY12797 was added to the coculture system. (A, B) IFNγ released into the coculture supernatant was measured after 48 h. Data are mean/SD (n = 3 replicates). Data were fit using log(agonist) vs response—variable slope (four parameters) in GraphPad Prism V.8.4.3. (C) BCY11864 increases the numbers of cytotoxic CD8+ T cells in contrast to vehicle and monomethyl auristatin E (MMAE). MC38-Nectin-4 tumors injected with vehicle, BCY11864, and MMAE were evaluated for the presence of cytotoxic T cells (CD8+/GzB+) by immunohistochemistry (IHC) 24 h after microinjection. Pink: CD8; aqua: GzB; yellow: fluorescent tracking marker FTM; blue: nucleus (4',6-diamidino-2-phenylindole (DAPI)). (D) Quantitation of double positive CD8+/GzB+ cells from tumor tissues normalized to total CD8+ cells. **$p < 0.001$, one-way ANOVA with Dunnett's post-test.

Functional Activity of *Bicycle* TICAs against Primary Immune Cells. The HT1376/CD137 reporter coculture assay system enabled us to quickly screen many *Bicycle* TICAs as the first filter in our screening cascade. To confirm that this activity translated to primary human immune cells, HT1376 tumor cells were cocultured with human peripheral blood mononuclear cells (PBMCs) from healthy donors and treated with anti-CD3 to stimulate CD137 expression on immune cells. Key molecules at each stage of the optimization campaign were evaluated in this assay. BCY8854, BCY10000, BCY10572, BCY11385, BCY11864, BCY12587 (Figure 6A) and BCY11863[24] all led to a dose-dependent increase in secretion of proinflammatory cytokines IFNγ and IL-2 (Table S3). This experiment was repeated in multiple donors: BCY11863 and its close analogue BCY11385 were the two most potent *Bicycle* TICAs in this assay (Table S3). No IL-2 or IFNγ secretion was observed with BCY13144, a 1:2 *Bicycle* TICA, where the Nectin-4 *Bicycle* was modified by replacing two tryptophans with their corresponding D-enantiomers to abrogate binding to Nectin-4. Surprisingly, the potency of BCY12587 in the primary immune cell assay was about 10-fold lower compared to the reporter assay coculture system. We hypothesize that the reduced affinity of the CD137 *Bicycle* incorporated in BCY12587 (1:2 Nectin-4/CD137

valency) to its target is masked by avidity effects of the dimeric CD137 moiety in the overexpressing CD137 reporter system. But in activated primary immune cells that have more physiologically relevant levels of CD137, the avidity effects may be diminished highlighting the need to evaluate these *Bicycle* TICAs in assays using a physiologically relevant immune cell population.

In Vivo Pharmacodynamics of a *Bicycle* TICA after Intratumoral Microdosing. We sought to next evaluate the pharmacodynamics of the Nectin-4/CD137 *Bicycle* TICAs in vivo. We used BCY11864 (1:2 format) as a tool compound for this purpose. We first confirmed that BCY11864 was functionally active in PBMCs (stimulated with anti-CD3) cocultured with the Nectin-4-expressing clone of murine colon adenocarcinoma cells (MC38-Nectin-4) to be used in the in vivo model (Figure 6B).

The effect of BCY11864 in Nectin-4-overexpressing MC38 tumor microenvironment was then explored in huCD137 C57Bl/6 mice using the comparative in vivo oncology (CIVO) platform.[28] The CIVO platform operates by injecting microdoses of drugs directly into accessible tumor tissues in trackable columns, where tissues can be analyzed after resection for the effect of the drug treatment in the tumor. MC38-Nectin-
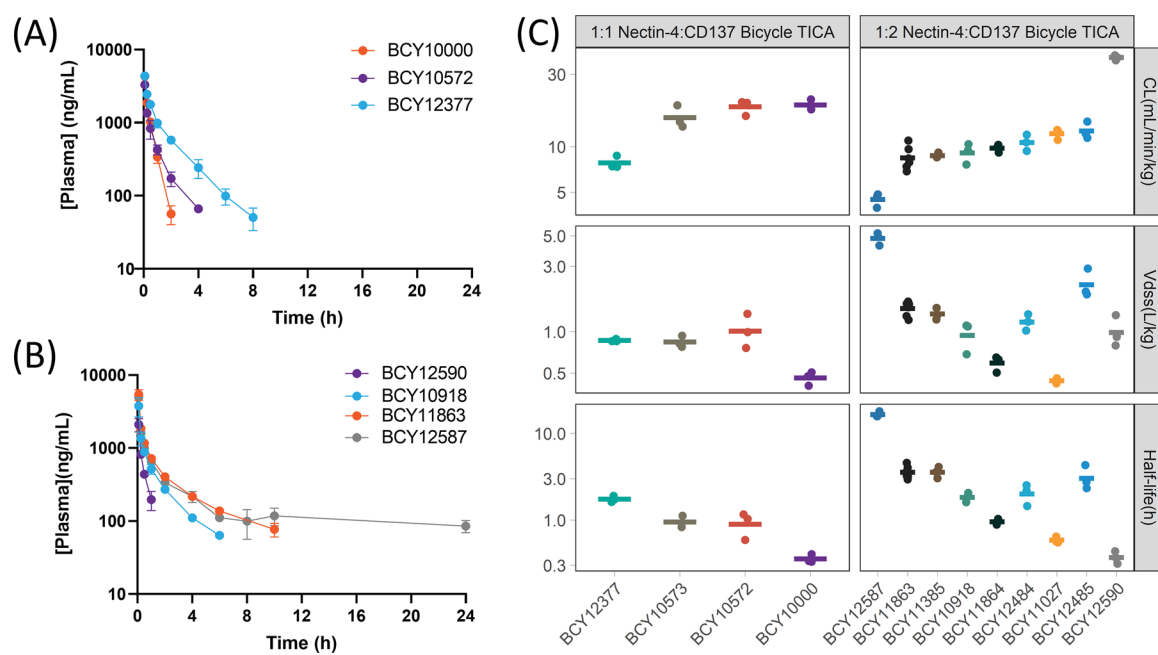
Figure 7. Characterization of pharmacokinetics of the Nectin-4/CD137 *Bicycle* TICAs in rats. (A) Plasma concentration−time profile of representative 1:1 Nectin-4/CD137 *Bicycle* TICAs BCY10000, BCY10572, or BCY12377 after being dosed intravenously (IV, bolus) at 2 mg/kg in SD rats. (B) Plasma concentration−time profile of representative 1:2 Nectin-4/CD137 *Bicycle* TICAs BCY12590, BCY10918, BCY11863, or BCY12587 after being dosed intravenously (IV, bolus) at 2 mg/kg in SD rats. (A, B) Data are mean ± SD (n = 3 animals/compound). (C) Clearance (CL), volume of distribution at a steady state (V_{dss}) and resulting terminal half-life for all Nectin-4/CD137 *Bicycle* TICAs assessed for pharmacokinetics in SD rats. Mean values are shown using crossbar with individual animal data as points on the plot.

4 tumors were microdosed with vehicle, the microtubule inhibitor monomethyl auristatin E (MMAE) and BCY11864 and analyzed 24 h later for CD8 and Granzyme B (GzB) expression by immunohistochemistry (IHC). An increase in the proportion of CD8+/GzB+ double positive cells of total CD8+ cells was observed in BCY11864 injection sites compared to the vehicle or MMAE injection sites demonstrating a significant increase in cytotoxicity of the CD8+ T-cell population (Figure 6C,D). Interestingly, the increase in GzB+ cells by BCY11864 was not limited to CD8+ cells, indicating that BCY11864 treatment can activate other cytotoxic cell types beyond CD8+ T cells in tumor tissues either directly or indirectly. The identity of the other GzB+ cells is still unknown. The in vitro and in vivo studies with BCY11864 demonstrate that immunomodulation with Nectin-4/CD137 *Bicycle* TICAs is consistent with the mechanism of CD137 co-stimulation.

Optimization of Pharmacokinetics. Bicyclic peptides are generally characterized by relatively short-circulating half-lives and rapid, renal elimination. However, unlike biologics, the pharmacokinetic parameters of these compounds can be tuned using medicinal chemistry. To elucidate the impact of medicinal chemistry on the pharmacokinetics of the *Bicycle* TICAs, key molecules from each round of chemical optimization were evaluated in Sprague-Dawley (SD) rats.

The plasma concentration−time profiles of the *Bicycle* TICAs in SD rats after IV bolus administration demonstrate a range of different in vivo exposure profiles that were obtained during the lead optimization process (Figure 7). The 1:1 compound BCY10000 had a clearance (CL) of 19 mL/kg/kg with a half-life of 0.36 h when dosed intravenously (Figure 7A−C). Replacement of the Sar10-PEG12 linker (linker 1, Figure 2B) with a shorter PEG5 linker (linker 3, Figure 2B) improved the half-life of the resulting molecule BCY10573 to 0.96 h. Moving the attachment point in the CD137 *Bicycle* (BCY11014 →

BCY8928, Table S7) from the C-terminal residue (Dap— BCY10573) to a position central to loop 1 (dLys4— BCY10572) did not result in a change to the CL (18 mL/min/kg) or half-life (0.93 h). Removal of the C-terminal alanine residue of the CD137 *Bicycle* from BCY10572 along with a Pro to Glu substitution at position 2 (BCY12377) resulted in a decrease in the CL of twofold to 7.8 mL/min/kg with an increase in terminal half-life to 1.8 h (Figure 7A). BCY10918, the initial 1:2 Nectin-4/CD137 *Bicycle* TICA containing a trimesic acid hinge and PEG10 linker (hinge 1, Figure 4A), but the same Nectin-4 and CD137 *Bicycles* as the 1:1 BCY10572 had a CL of 9.1 mL/min/kg and half-life of 1.8 h (Figure 7B,C). Replacing the trimesic acid hinge with another trifunctional linker (tri(carboxyethyloxyethyl)amine) (hinge 2, Figure 4A, BCY11027) decreased the half-life to 0.59 h.

A series of 1:2 compounds that incorporated the simple and commercially available hinge 5 (*N*-(acid-PEG3)-*N*-bis(PEG3-azide)) (Figure 5) were also evaluated. BCY11864, with the lower affinity CD137 *Bicycle* (BCY7744, Table S7) exhibited a half-life of 0.95 h. Replacing the CD137 binder with the higher affinity BCY8928 (Table S7) led to BCY11863, which had a CL of 8.5 mL/min/kg and a terminal half-life of 3.6 h, significantly extended over BCY11864. Other modifications to BCY11863 such as changing the attachment point on the CD137-binding *Bicycle* to the C-terminal Dap residue (BCY11385), removing the C-terminal alanine from the CD137-binding *Bicycle* (BCY12485) or removing the C-terminal alanine and substituting Pro for Glu at position 2 (BCY12484) did not significantly change the CL or half-life compared to BCY11863.

Replacing D-Asp3 and Asp6 on the Nectin-4 *Bicycle* in BCY11863 to D-Glu and Glu (BCY12590), respectively, increased the clearance from 7.7 to 39 mL/min/kg resulting in a half-life of only 0.37 h. Removal of the C-terminal alanine and replacement of N-terminal acetylated cysteine to 3-
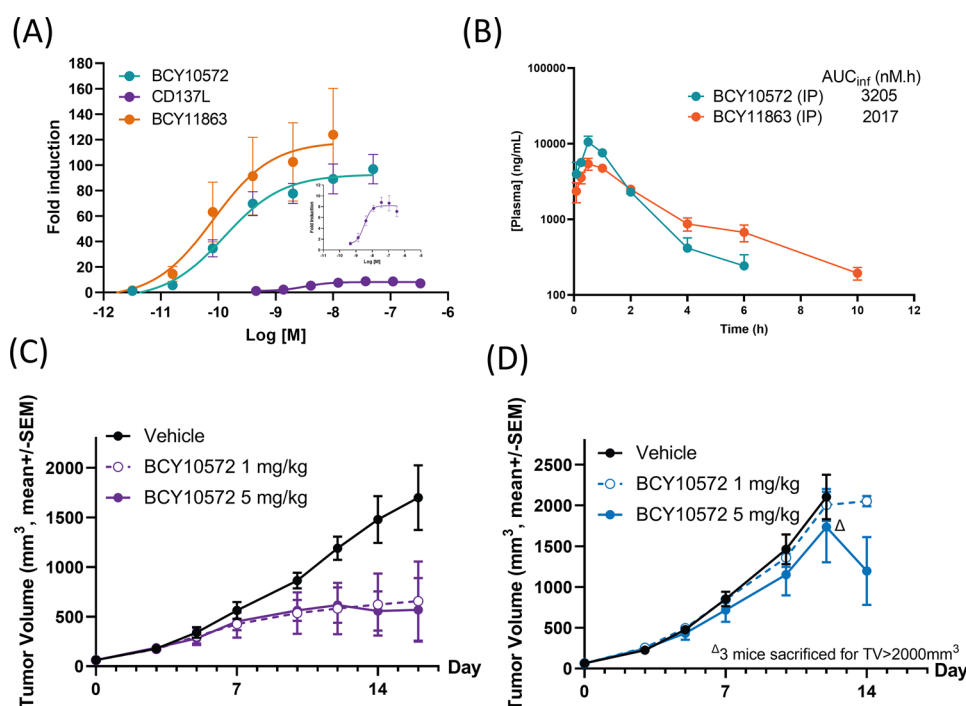
Figure 8. Nectin-4/CD137 *Bicycle* TICA cause tumor regression in vivo. (A) Jurkat-CD137 reporter cells were cocultured with CT26 clone overexpressing Nectin-4 (CT26-Nectin-4) and treated with BCY10572 (1:1 *Bicycle* TICA), BCY11863 (1:2 *Bicycle* TICA), or CD137L. Data are mean ± s.d. ($n \geq 3$ replicates). (B) Plasma concentration of BCY10572 and BCY11864 when dosed at 15 mg/kg by intraperitoneal injection to CD-1 mouse. (C, D) CT26-Nectin-4 tumor-bearing huCD137-Balb/c (C) or wild type Balb/c (D) mice were treated with daily doses of vehicle or BCY10572 (1 or 5 mg/kg) and tumor growth was monitored. Data are mean ± standard error of the mean (SEM) ($n = 5$ mice/treatment cohort). TV: tumor volume.

mercaptopropanoic acid (BCY12587) in BCY11863 decreased the CL to 4.5 mL/min/kg and increased the half-life to 17 h (Figure 7B,C).

The plasma protein binding of selected molecules was also characterized by ultracentrifugation to determine free drug concentrations in vivo as well as to calculate unbound CL and volume of distribution at steady state (Table S4). The Nectin-4 *Bicycle* TICAs exhibited moderate plasma protein binding with an unbound fraction in plasma ($f_{u,p}$) ranging from 0.088 to 0.37. Analysis of unbound pharmacokinetic parameters indicates that increases in half-life are primarily driven by increases in unbound V_{dss} of the *Bicycle* TICAs.

Characterization of Solubility. High solubility of drug candidates is desirable as it can reduce formulation challenges and enable more flexibility in clinical dosing strategies. Both BCY10572 (1:1, 29 mg/mL) and BCY11863 (1:2, 20 mg/mL) had high thermodynamic solubility in 50 mM phosphate buffer at pH 7.4 while the solubility of BCY12587 was found to be much lower (3.1 mg/mL).

Antitumor Activity in Mouse Models. BCY10572 and BCY11863 were selected for further characterization in efficacy studies because they represented two different classes of the *Bicycle* TICAs (1:1 and 1:2 format respectively), and both had good solubility.

The Nectin-4 *Bicycle* (BCY8116) binds to mouse, rat, monkey, and human Nectin-4, however, the CD137-binding *Bicycle* (BCY8928) binds only to human and monkey CD137. BCY10572 (1:1 *Bicycle* TICA) antitumor activity was initially evaluated in either wild-type (wt) Balb/c or huCD137-Balb/c (with knock-in of the extracellular domain of human CD137) mice bearing Nectin-4-expressing CT26 (CT26-Nectin-4) tumors. Both compounds were first evaluated with the in vitro CD137 reporter coculture assay to confirm that CD137

activation would be achieved with the CT26-Nectin-4 cell line (Figure 8A). The pharmacokinetic profiles of both compounds after intraperitoneal (IP) dosing were assessed in CD-1 mice and found to be similar (Figure 8B).

Potent antitumor activity was observed in huCD137-Balb/c mice with 1 and 5 mg/kg daily (QD) intraperitoneal (IP) dosing of BCY10572. Unsurprisingly, no BCY10572 antitumor activity was observed in wt Balb/c mice due to the lack of cross-reactivity to mouse CD137 (Figure 8C,D). BCY11863 (1:2) was also evaluated in the CT26-Nectin-4/huCD137 mouse model and, at 5 mg/kg QD, significant antitumor activity was observed.[24] Based on these preliminary in vivo activity results, both compounds were further profiled to identify the lead candidate.

Characterization of the Pharmacokinetics in Nonhuman Primates (NHPs). To identify a final candidate molecule, the translatability of the pharmacokinetics of BCY10572 and BCY11863 from rodents to higher species was evaluated in cynomolgus monkeys. Each compound was infused for 30 min in NHPs ($n = 2$ animals/compound) at a dose of 1 mg/kg. BCY10572 had a mean plasma clearance of 30 mL/min/kg and a V_{dss} of 0.6 L/kg, resulting in half-life of 0.5 h. The high clearance of BCY10572 was not predicted from pharmacokinetics in rats. BCY11863, on the other hand, had a plasma clearance of 3.3 mL/min/kg and a V_{dss} of 0.6 L/kg, resulting in a terminal half-life of 5.3 h in this study (Figure 9A). Pharmacokinetic data from follow-up studies of BCY11863 in NHPs are described elsewhere.[24] BCY11863 exhibited linear pharmacokinetics in doses ranging from 1 to 30 mg/kg in mouse, enabling the development of exposure-response models in the preclinical efficacy models (Figure 9B).

The mean PK parameters of BCY11863 from multiple studies scaled well across the preclinical species (Figure 9C and Table S5), supporting an allometric scaling approach for human PK
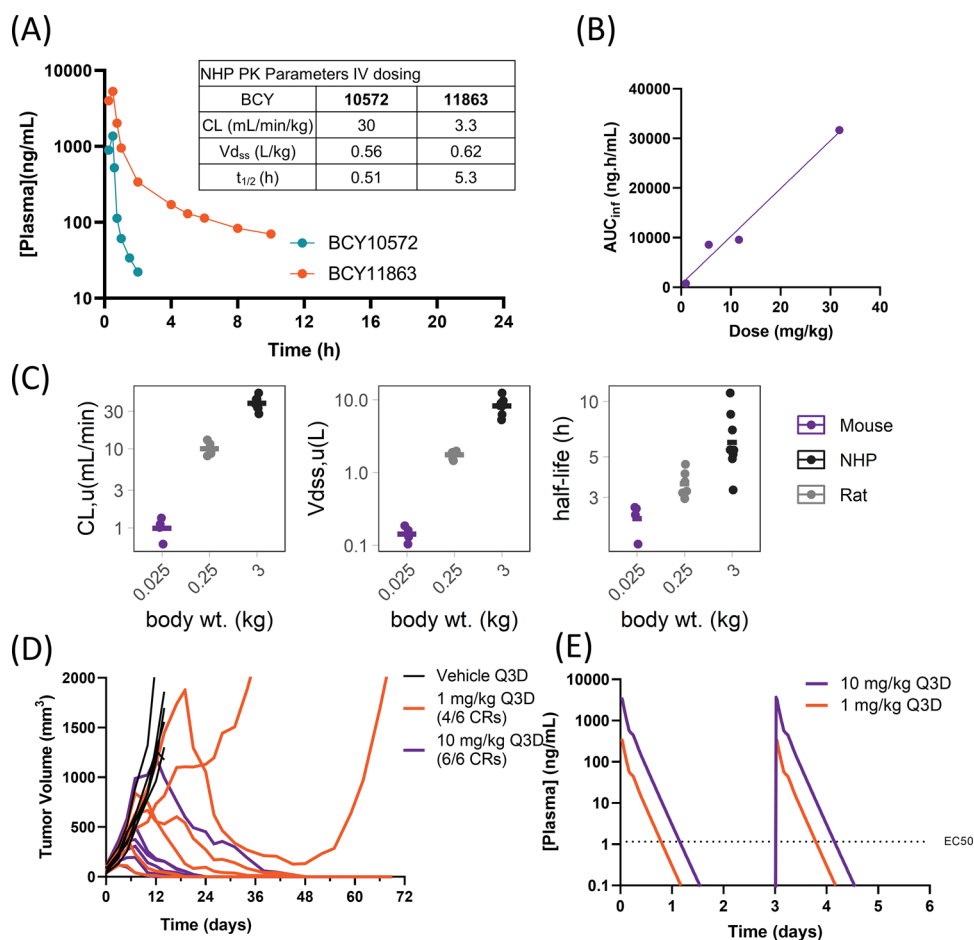
Figure 9. *Bicycle* TICA pharmacokinetics across preclinical species and antitumor activity in the MC38 syngeneic model. (A) Plasma concentration−time profile and pharmacokinetic parameters (table insert) after infusion of 1 mg/kg of BCY10572 or BCY11863 over 30 min in NHPs (cynomolgus monkeys). Data are mean ($n = 2$ animals/compound). (B) Exposure (AUC_{inf}) of BCY11863 plotted as a function of dose after administration of 1, 5, 10, and 30 mg/kg nominal dose of BCY11863 in CD-1 mice. (C) Unbound clearance (CL), volume of distribution (V_{dss}), and terminal half-life of BCY11863 plotted against mean body weight (wt) of mouse ($n = 4$), rat ($n = 6$), and NHPs ($n = 8$). (D) MC38-Nectin-4 tumor growth in huCD137 C57Bl/6 mice with Q3D dosing of vehicle or BCY11863 ($n = 6$/cohort, last dose given on day 15). The number of complete responders (CRs) is indicated in the figure. (E) Simulated plasma concentration−time profile of BCY11863 after multiple doses at 1 and 10 mg/kg Q3D in mice.

prediction. Based on these findings, BCY11863 was selected as the lead candidate.

Further Characterization of Candidate BCY11863. As the lead *Bicycle* TICA candidate, BCY11863 was more extensively profiled in vitro and in vivo.[24] In additional studies using the CT26 model described earlier, it was observed that the antitumor activity for BCY11863 could be achieved even when dosed Q3D.[24] This indicated that a positive pharmacologic effect with *Bicycle* TICAs can be achieved without sustained plasma concentrations, which is markedly different from the exposure approaches taken with the recombinant bispecific CD137 agonists currently under clinical development. The reasonably short-circulating half-life of BCY11863 in mice (Figure 8B, 2.3 h after IP injection) therefore permits a further exploration of the effect of intermittent plasma exposure on antitumor activity.

Mice bearing subcutaneous MC38-Nectin-4 tumors were treated with BCY11863 at 1 and 10 mg/kg Q3D IP. BCY11863 was efficacious, reducing tumor growth and inducing complete responses (CRs) with the rate of CRs ranging from 4/6 (1 mg/kg Q3D) to 6/6 (10 mg/kg Q3D) by day 40 (Figure 9D). The plasma concentration−time profiles for BCY11863 dosing regimens in mice were simulated to assess the amount of time

in a dosing cycle that the concentration was maintained at or above the average EC50 required to induce IFNγ and IL-2 secretion (Figure 9E). The 1 mg/kg Q3D dosing regimen that led to robust efficacy had a plasma PK profile that maintained concentrations over EC50 for approximately 1 day out of a 3 days dosing cycle. Further extension of this work described elsewhere showed that a dosing regimen (5 mg/kg at 0 and 24 h) which would lead to nearly continuous target coverage over the first 2 days of the weekly dosing cycle also achieved maximum antitumor activity, however, longer exposures did not improve antitumor activity.[24] The potent target-dependent immune activation combined with translatable pharmacokinetics of BCY11863 in preclinical species and robust antitumor immunity achieved with intermittent dosing in mouse efficacy models supports once a week dosing in the clinic.

■ DISCUSSION AND CONCLUSIONS

Synthetic and low-molecular-weight tumor-targeted immune agonists represent a unique opportunity to create differentiated molecules that can be chemically tuned to achieve different structural and functional properties. These tunable attributes mean that compounds can be optimized to elicit the desired pharmacology and to create a molecule that has sufficiently

strong pharmaceutical properties to warrant advancement to clinical development. Our goal was to discover a Nectin-4-targeted CD137 agonist clinical candidate that had the optimal in vivo characteristics to elicit the desired immune cell response by co-ligating Nectin-4 and CD137 and that could be dosed once a week in the clinic. To this end, we deployed a multipronged approach to optimize the affinity to both targets, linker length, binder stoichiometry, solubility, and pharmacokinetic properties.

The in vitro structure−activity relationships of the 1:1 Nectin-4/CD137 *Bicycle* TICAs elucidated the rules for modulating potency, with affinity to the tumor antigen having the largest impact as compared to the affinity to the co-stimulatory receptor. Given the complex structures of other bispecific modalities, a general lack of sensitivity of the potency to linker length was a surprising finding. This lack of sensitivity to linker length may be specific for BCY8116 binding to Nectin-4, and this result may not translate to another *Bicycle*-based tumor-targeted immune cell agonist. However, it is intriguing to speculate that the small size and relative flexibility of linkers may permit tuning of the distance between both target proteins at the synapse between tumor and immune cells in a manner that may be more challenging to achieve with larger recombinant protein modalities. By exploring the valency of the *Bicycles*, it was demonstrated that the 1:2 format (Nectin-4/CD137) was the optimal balance of potency, E_{max}, target dependency, and manufacturing feasibility. We are currently exploring these structure−activity parameters in the context of other *Bicycle* tumor-targeted immune cell agonists, which will test the generality of these observations.

We previously described *Bicycle* toxin conjugates (BTCs) that have short plasma half-lives but have profound antitumor activity in vivo with a weekly dosing regimen.[18] The most likely basis for this result is that the pharmacokinetic and functional properties lead to rapid delivery of the toxin payload MMAE in the tumor where it is retained. For the *Bicycle* tumor-targeted immune cell agonists, we hypothesized that the co-engagement of Nectin-4 and CD137 and activation of the immune response would require relatively longer exposures compared to BTCs because the *Bicycle* TICA functions by providing a signal to tumor-infiltrating immune cells that require some duration of action rather than deposition of a payload, which can, in principle, occur in a very short time. Common approaches for modulating the pharmacokinetics of peptide-based therapeutics include lipidation, pegylation, or extended-release formulations.[15,29−31] Pegylation to extend half-life requires conjugation to relatively high MW PEGs (20−40 kDa), and this would significantly increase the size of the *Bicycle* TICA and could limit tumor penetration, a key design feature of the *Bicycle* TICAs. Lipidation can increase half-life and can encourage high tumor uptake.[32] This approach was not pursued due to a risk of nontumor targeted CD137 activation mediated by nonspecific tissue binding and because hydrophobicity can increase biodistribution to the liver, where CD137 agonism presents severe hepatotoxicity risks.[33] Therefore, the impact of structural changes to the bicyclic peptides and the linkers was evaluated to determine if a suitable PK profile could be attained without the need to append half-life extending moieties. Analysis of the pharmacokinetic data from the Nectin-4/CD137 *Bicycle* TICA series showed (Table S4) that the molecules with longer half-lives were driven mostly by higher unbound volume of distribution with differences in unbound CL being more subtle.

BCY10572 and BCY11863 were deemed suitable for candidate consideration since they had good potency and exposure based on rodent studies. BCY10572 is a 1:1 Nectin-4/CD137 *Bicycle* TICA with nanomolar potency; BCY11863 is a 1:2 Nectin-4/CD137 *Bicycle* TICA with subnanomolar potency. BCY10572 showed a very high clearance in NHPs (Figure 9A). This combined with its slightly weaker in vitro potency (Tables S2, and S3) and the observed translatability of the pharmacokinetic profile and robust antitumor activity of BCY11863 with an intermittent dosing schedule in MC38-Nectin-4 syngeneic mouse models led to nomination of BCY11863 as the developmental candidate.[24] BCY11863 allows us to explore the potential of a short-acting CD137 agonist in the clinic, which then differentiates it from other modalities, addressing this target with a tumor-targeted bispecific approach.

We believe that transient but potent agonism of CD137 (and other tumor necrosis factor receptor (TNFR) family members) may be superior to prolonged receptor agonism. Based on recent clinical data, maintaining a persistently high level of target engagement in bispecific modalities may lead to ineffective signaling and lead to a suboptimal immune response.[34] If this is the case, this opens up the possibility of using *Bicycles* with superior tissue penetration and short-circulating exposure to target other co-stimulatory receptors (e.g., OX40) in this class that have failed in the clinic, possibly due to the physiochemical properties of the drug. In contrast to both the second generation of tumor-targeted and nontargeted CD137 agonists undergoing clinical development, this approach may achieve the perfect balance of potent tumor-localized activity and short peripheral exposure to drive efficacy while providing a wider safety margin and preventing overstimulation and activation-induced cell death of the immune cells.

As a clinical candidate, BCY11863 was renamed BT7480, an homage to the phage clones from which it originated. It presents us with the opportunity to explore a differentiated molecule against a promising target in a crowded therapeutic space that has the potential to positively impact patients' lives.

■ EXPERIMENTAL SECTION

Methods for synthesis and purification of *Bicycle* TICAs can be found in the Supporting Information. Lead compounds including those used in in vivo efficacy studies were >95% purity as measured by high-performance liquid chromatography (HPLC). All compounds had purities of >90% by HPLC with one exception noted in Table S8. The HPLC traces of all *Bicycle* TICAs used in in vivo efficacy and ADME studies are available in the Supporting Information.

Cell Lines and Reagents. HT1376, NCI-H292, PC3, and CT26 cells were obtained from ATCC (American Type Culture Collection). MC38 cells were obtained from the National Cancer Institute (L-159-2018/1). CT26 and MC38 cells were engineered to express mouse Nectin-4 (NM_027893.3) as described.[21] Human peripheral blood mononuclear cell (PBMC) isolation was described.[21]

Recombinant proteins: human CD137 (92 204B, R&D Systems) and human CD137L (2295-4L-025, R&D Systems) were purchased. Human Nectin-4 (residues 32−349) and rat Nectin-4 (residue 31−347) with a gp67 signal sequence and C-terminal FLAG tag were cloned into pFastbac-1 and baculovirus using standard Bac-to-Bac protocols (Life Technologies). Sf21 cells at 1×10^6 mL^{-1} in Excell-420 medium (Sigma) at 27 °C were infected at a multiplicity of infection (MOI) of 2 with a P1 virus stock for protein expression. The supernatant was harvested at 72 h and incubated for 1 h at 4 °C with anti-FLAG M2 affinity agarose resin (Sigma) followed by a phosphate-buffered saline (PBS) wash. Resin was subsequently transferred to a column and washed extensively with phosphate-buffered saline (PBS). Protein was eluted with 100 μg/mL FLAG peptide concentrated to a

volume of 2 mL and loaded onto an S-200 Superdex column (GE Healthcare) in PBS at 1 mL/min. 2 mL fractions were collected and fractions containing Nectin-4 protein were concentrated.

CD137 Reporter Coculture Assays. CD137 bioassay kits (Promega) were carried out according to the manufacturer's protocol. Briefly, a Jurkat T-cell line engineered to express human CD137 and a luciferase reporter driven by a response element that can respond to CD137 ligand/agonist antibody stimulation were cultured at 37 °C, 5% CO$_2$ for 6 h with or without test article in coculture with 10,000 cells of indicated tumor cell line. After 6 h, the Bio-Glo Luciferase reagent was added to each well. Luminescence was measured on a BMG CLARIOStar microplate reader. Fold induction was calculated as relative light unit (RLU) divided by RLU of background (no test article) wells.

Surface Plasmon Resonance (SPR) Assay. CD137: SPR experiments were performed on a Biacore T200 to determine the k_a (M^{-1} s^{-1}), k_d (s^{-1}), and K_D (nM) values of peptides binding to human CD137 protein. Recombinant human CD137 (R&D systems) was resuspended in PBS and biotinylated using an EZ-Link Sulfo-NHSLC-LC-Biotin reagent (Thermo Fisher) as per the manufacturer's suggested protocol. The protein was desalted to remove uncoupled biotin using spin columns into PBS. Streptavidin was immobilized onto a XanTec CMD500D chip and biotinylated CD137 in PBS/0.05% Tween 20 captured to a level of 800−1800 RU. A dilution series of the peptides were prepared in PBS/0.05% Tween 20 with a final dimethyl sulfoxide (DMSO) concentration of 0.5%. The top peptide concentration was 500 nM or 10 μM with 6 further threefold (500 nm), or twofold (10 μM) dilutions in PBS/0.05% Tween 20. The peptides were injected over the chip at 25 °C at a flow rate of 90 μL/min with 60 s association and 100−600 s dissociation. After each cycle, a regeneration step (10 μL of 10 mM glycine pH 2) was employed. Data were corrected for DMSO excluded volume effects. All data were double referenced for blank injections and reference surfaces using standard processing procedures and data processing and kinetic fitting were performed using Scrubber software, version 2.0c (BioLogic Software). Data were fitted using a mass transport model allowing for mass transport effects where appropriate.

Nectin-4: SPR experiments were performed on a Biacore T200 instrument to determine the k_a (M^{-1} s^{-1}), k_d (s^{-1}), K_D (nM) values of peptides binding to a recombinant human Nectin-4 protein. The protein was randomly biotinylated in PBS using the EZ-Link Sulfo-NHS-LC-LC-Biotin reagent (Thermo Fisher) as per the manufacturer's suggested protocol. The protein was extensively desalted to remove uncoupled biotin using spin columns into PBS. Streptavidin was immobilized on a CM5 chip (GE Healthcare) and biotinylated Nectin-4 in PBS/0.05% Tween 20 captured to a level of 1200−1800 RU. A dilution series of the peptides were prepared in PBS/0.05% Tween 20 with a final DMSO concentration of 0.5%. The top peptide concentration was 100 nM with 6 further twofold dilutions. The peptides were injected over the chip at 25 °C at a flow rate of 50 μL/min with 60 s association and dissociation between 400 and 1200 s depending upon the individual peptide. Data were corrected for DMSO excluded volume effects. All data were double referenced for blank injections and reference surfaces using standard processing procedures and data processing and kinetic fitting were performed using Scrubber software, version 2.0c (BioLogic Software). Data were fitted using a simple 1:1 binding model allowing for mass transport effects where appropriate.

Cytokine Secretion Assays and Cytokine Quantification. Frozen PBMCs from healthy human donors were thawed and washed one time in room-temperature PBS with benzonase and then resuspended in RPMI supplemented with 10% heat-inactivated fetal bovine serum, 1× penicillin/streptomycin, 10 mM HEPES, and 2 mM L-glutamine (herein referred to as R10 medium). Mouse (MC38 or MC38-Nectin-4) or human (HT1376) tumor cells were cultured in the appropriate media. One hundred microliters of PBMCs (1 × 10^6/mL) and 100 μL of tumor cells (1 × 10^5/mL) (effector/target cell ratio 10:1) were plated in each well of a 96-well flat bottom plate for the coculture assay. A soluble anti-CD3 mAb (100 ng/mL, clone OKT3; Biolegend) was added to the culture on day 0 to stimulate human PBMCs. Test,

control compounds, or vehicle controls were diluted in R10 media and 50 μL was added to respective wells to bring the final volume per well to 250 μL. Plates were covered with a breathable film and incubated in a humidified chamber at 37 °C with 5% CO$_2$ for 2 days. Supernatants were collected 24 and 48 h after stimulation, and human interleukin-2 (IL-2) and interferon gamma (IFNγ) were detected by Luminex. Briefly, the standards and samples were added to a black 96-well plate. A microparticle cocktail (provided in Luminex kit, R&D Systems) was added and shaken for 2 h at room temperature. The plate was washed three times using a magnetic holder. Biotin cocktail was then added to the plate and shaken for 1 h at room temperature (RT). The plate was washed three times using a magnetic holder. Streptavidin cocktail was added to the plate and shaken for 30 min at RT. The plates were washed three times using a magnetic holder, resuspended in 100 μL of wash buffer, shaken for 2 min at RT, and read using the Luminex 2000. Raw data were analyzed using built-in Luminex software to generate standard curves and interpolate protein concentrations, and all other data analyses and graphing were performed using Excel and Prism software.

CIVO. A mouse microdosing study was performed in C57BL/6J-hCD137 mice (B-hTNFRSF9(CD137); Biocytogen, Beijing, China) with subcutaneously implanted Nectin-4-overexpressing (MC38-Nectin-4) tumors (21). Three anesthetized MC38-Nectin-4 tumor (around 860 mm^3) bearing mice were microdosed transcutaneously with a 2 μL injection volume of vehicle (25 mM histidine, 10% sucrose pH 7), 120 μM MMAE, and 1.85 μM BCY11864 using the CIVO device. Inert fluorescent injection tracking microspheres (FTMs) were added to each needle. Mice were sacrificed 24 h after dosing, and tumors were fixed with 10% neutral buffered formalin and processed for paraffin embedding for IHC analysis. Fluorescent IHC analysis was performed for CD8 (clone D4W2Z; Cell Signaling #98941) and GrzB (clone 16G6, Thermo Fisher #14-8822) and nuclear staining was done with DAPI (Invitrogen #D3571). Images were acquired to capture CD8-, GrzB-, and nuclear staining alongside with the FTM, indicating the injection path.

Pharmacokinetics. Male Sprague-Dawley rats were dosed with 2 mg/kg (IV bolus) of *Bicycle* TICA. Male CD-1 mice were dosed at 15 mg/kg BCY11863 or BCY10572 intraperitoneally. Male naïve cynomolgus monkeys were administered with a 30 min intravenous infusion of 1 mg/kg BCY11863 or 1 mg/kg BCY10572. The *Bicycle* TICAs were formulated in 25 mM histidine HCl, 10% sucrose pH 7. Serial bleeding was performed, and all blood samples were immediately transferred into prechilled microcentrifuge tubes containing 2 μL K2-EDTA (0.5 M) as an anticoagulant and placed on wet ice. Blood samples were immediately processed for plasma by centrifugation at approximately 4 °C, 3000g. The precipitant including internal standard was immediately added into the plasma, mixed well, and centrifuged at 12,000 rpm, 4 °C for 10 min. The supernatant was transferred into prelabeled polypropylene microcentrifuge tubes and then quick-frozen over dry ice. The samples were stored at 70 °C or below as needed until analysis. The supernatant samples (7.5 μL) were directly injected for liquid chromatography−tandem mass spectrometry (LC−MS/MS) analysis using an Orbitrap Q Exactive in positive ion mode to determine the concentrations of *Bicycle*. Plasma concentration vs time data were analyzed by noncompartmental analysis (NCA) using the Phoenix WinNonlin 6.3 software program.

Plasma Protein Binding. The plasma protein binding of *Bicycle* TICAs was measured using ultracentrifugation as previously described.[35]

Syngeneic Tumor Models. Mouse efficacy studies were performed in C57BL/6J-hCD137 mice (B-hTNFRSF9(CD137); Biocytogen, Beijing, China) with subcutaneously implanted MC38-Nectin-4 tumors or in BALB/c hCD137 and BALB/c WT mice (GemPharmatech, Nanjing, China) with subcutaneously implanted CT26-Nectin-4 tumors (21).

MC38-Nectin-4 tumor-bearing mice were randomized into treatment groups when average tumor volumes reached 72 mm^3 and were treated with vehicle (25 mM histidine, 10% sucrose, pH 7) or BCY11863 at 1 or 10 mg/kg every 3 days (Q3D ×6). CT26-Nectin-4 tumor-bearing mice were randomized into treatment groups when

average tumor volumes reached 68 mm^3 (in BALB/c huCD137-mice) or 64 mm^3 (in WT BALB/c-mice) and were treated with vehicle (25 mM histidine, 10% sucrose, pH 7) or BCY10572 at 1 or 5 mg/kg daily until day 15 (BALB/c huCD137-mice) or day 14 (WT BALB/c mice). Tumor growth was monitored by caliper measurements. Tumor volume is expressed in mm^3 using the formula: $V = 0.5a \times b^2$, where a and b are the long and short diameters of the tumor, respectively. All treatments were administered intraperitoneally (IP).

All of the procedures related to animal handling, care, and treatment in the studies were performed according to the guidelines approved by the Institutional Animal Care and Use Committee of Presage Biosciences (Seattle, WA) or WuXi AppTec (Beijing, China), following the guidance of the Association for Assessment and Accreditation of Laboratory Animal Care.

Simulation of PK for Dosing Regimens in MC38 Syngeneic Model Efficacy Studies. The plasma concentration−time profiles after intraperitoneal administration of BCY11863 in CD-1 mice were analyzed using a two-compartment model (2C) in Phoenix Winnonlin. The mean PK parameters from the 2C model were used to simulate the plasma concentration−time profiles for the doses and dosing regimens in the in vivo efficacy study.

ASSOCIATED CONTENT

Supporting Information

The Supporting Information is available free of charge at https://pubs.acs.org/doi/10.1021/acs.jmedchem.2c00505.

General synthesis methods for bicyclic peptides, conjugation of 4-penynoic acid to bicyclic peptides, *Bicycle* TICAs; synthesis methods for BCY9499, BCY9400, BCY10917, BCY11027, BCY11022, and BCY12970; sensorgrams for *Bicycle* TICAs incorporating weak CD137 binders in 1:1 and 1:2 format; tables containing binding affinities to Nectin-4 and CD137, EC50 and E_{max} in CD137 reporter assay, EC50 in PBMC coculture assay, pharmacokinetics in SD rats, mean PK parameters for BCY11863, composition of the Nectin-4/CD137 *Bicycle* TICA, sequence of Nectin-4 and CD137 bicyclic peptides, % purity and m/z of *Bicycle* TICAs; HPLC traces of *Bicycle* TICAs used in in vivo studies; structures of *Bicycle* TICAs described in this study; and references (PDF)

Molecular formula strings of all *Bicycle* TICAs along with associated biochemical and biological data (CSV)

AUTHOR INFORMATION

Corresponding Author

Nicholas Keen − *Bicycle Therapeutics, Lexington, Massachusetts 02421, United States*; Email: Nicholas.keen@bicycletx.com

Authors

Punit Upadhyaya − *Bicycle Therapeutics, Lexington, Massachusetts 02421, United States*; orcid.org/0000-0001-5439-201X

Julia Kristensson − *Bicycle Therapeutics, Cambridge CB22 3AT, U.K.*

Johanna Lahdenranta − *Bicycle Therapeutics, Lexington, Massachusetts 02421, United States*

Elizabeth Repash − *Bicycle Therapeutics, Lexington, Massachusetts 02421, United States*

Jun Ma − *Bicycle Therapeutics, Lexington, Massachusetts 02421, United States*

Jessica Kublin − *Bicycle Therapeutics, Lexington, Massachusetts 02421, United States*

Gemma E. Mudd − *Bicycle Therapeutics, Cambridge CB22 3AT, U.K.*; orcid.org/0000-0002-5075-1625

Lia Luus − *Bicycle Therapeutics, Lexington, Massachusetts 02421, United States*; orcid.org/0000-0003-1649-8416

Phil Jeffrey − *Bicycle Therapeutics, Cambridge CB22 3AT, U.K.*

Kristen Hurov − *Bicycle Therapeutics, Lexington, Massachusetts 02421, United States*

Kevin McDonnell − *Bicycle Therapeutics, Lexington, Massachusetts 02421, United States*

Complete contact information is available at:
https://pubs.acs.org/10.1021/acs.jmedchem.2c00505

ABBREVIATIONS USED

Bicycle TICA, *Bicycle* tumor-targeted immune cell agonist; BTC, *Bicycle* toxin conjugate; CIVO, comparative in vivo oncology; CD137L, CD137 ligand; CL, clearance; CR, complete responder; DARPins, designed ankyrin repeat proteins; EphA2, erythropoietin-producing hepatocellular receptor A2; Fabs, antigen-binding fragments; GzB, Granzyme B; IHC, immunohistochemistry; IFNγ, interferon gamma; IL-2, interleukin-2; IP, intraperitoneal; kDa, kilodalton; mAbs, monoclonal antibodies; NHP, nonhuman primate; MMAE, monomethyl auristatin E; PBMC, peripheral blood mononuclear cells; PK, pharmacokinetics; Q3D, once every 3 days; SPR, surface plasmon resonance; SD, Sprague-Dawley; TNFR, tumor necrosis factor receptors; V_{dss}, volume of distribution at steady state

REFERENCES

(1) Segal, N. H.; He, A. R.; Doi, T.; Levy, R.; Bhatia, S.; Pishvaian, M. J.; Cesari, R.; Chen, Y.; Davis, C. B.; Huang, B.; Thall, A. D.; Gopal, A. K. Phase I study of single-agent utomilumab (PF-05082566), a 4-1BB/CD137 agonist, in patients with advanced cancer. *Clin. Cancer Res.* **2018**, 24, 1816−1823.

(2) Segal, N. H.; Logan, T. F.; Hodi, F. S.; McDermott, D.; Melero, I.; Hamid, O.; Schmidt, H.; Robert, C.; Chiarion-Sileni, V.; Ascierto, P. A.; Maio, M.; Urba, W. J.; Gangadhar, T. C.; Suryawanshi, S.; Neely, J.;

Jure-Kunkel, M.; Krishnan, S.; Kohrt, H.; Sznol, M.; Levy, R. Results from an integrated safety analysis of urelumab, an agonist anti-CD137 monoclonal antibody. *Clin. Cancer Res.* **2017**, *23*, 1929−1936.

(3) Garber, K. Immune agonist antibodies face critical test. *Nat. Rev. Drug Discovery* **2020**, *19*, 3−5.

(4) Chester, C.; Sanmamed, M. F.; Wang, J.; Melero, I. Immunotherapy targeting 4-1BB: mechanistic rationale, clinical results, and future strategies. *Blood* **2018**, *131*, 49−57.

(5) Sanchez-Paulete, A. R.; Labiano, S.; Rodriguez-Ruiz, M. E.; Azpilikueta, A.; Etxeberria, I.; Bolanos, E.; Lang, V.; Rodriguez, M.; Aznar, M. A.; Jure-Kunkel, M.; Melero, I. Deciphering CD137 (4-1BB) signaling in T-cell costimulation for translation into successful cancer immunotherapy. *Eur. J. Immunol.* **2016**, *46*, 513−522.

(6) Chu, D. T.; Bac, N. D.; Nguyen, K. H.; Tien, N. L. B.; Thanh, V. V.; Nga, V. T.; Ngoc, V. T. N.; Anh Dao, D. T.; Hoan, L. N.; Hung, N. P.; Trung Thu, N. T.; Pham, V. H.; Vu, L. N.; Pham, T. A. V.; Thimiri Govinda Raj, D. B. An update on anti-CD137 antibodies in immunotherapies for cancer. *Int. J. Mol. Sci.* **2019**, *20*, 1822.

(7) Claus, C.; Ferrara, C.; Xu, W.; Sam, J.; Lang, S.; Uhlenbrock, F.; Albrecht, R.; Herter, S.; Schlenker, R.; Husser, T.; Diggelmann, S.; Challier, J.; Mossner, E.; Hosse, R. J.; Hofer, T.; Brunker, P.; Joseph, C.; Benz, J.; Ringler, P.; Stahlberg, H.; Lauer, M.; Perro, M.; Chen, S.; Kuttel, C.; Bhavani Mohan, P. L.; Nicolini, V.; Birk, M. C.; Ongaro, A.; Prince, C.; Gianotti, R.; Dugan, G.; Whitlow, C. T.; Solingapuram Sai, K. K.; Caudell, D. L.; Burgos-Rodriguez, A. G.; Cline, J. M.; Hettich, M.; Ceppi, M.; Giusti, A. M.; Crameri, F.; Driessen, W.; Morcos, P. N.; Freimoser-Grundschober, A.; Levitsky, V.; Amann, M.; Grau-Richards, S.; von Hirschheydt, T.; Tournaviti, S.; Molhoj, M.; Fauti, T.; Heinzelmann-Schwarz, V.; Teichgraber, V.; Colombetti, S.; Bacac, M.; Zippelius, A.; Klein, C.; Umana, P. Tumor-targeted 4-1BB agonists for combination with T cell bispecific antibodies as off-the-shelf therapy. *Sci. Transl. Med.* **2019**, *11*, No. eaav5989.

(8) Hinner, M. J.; Aiba, R. S. B.; Jaquin, T. J.; Berger, S.; Durr, M. C.; Schlosser, C.; Allersdorfer, A.; Wiedenmann, A.; Matschiner, G.; Schuler, J.; Moebius, U.; Rothe, C.; Matis, L.; Olwill, S. A. Tumor-localized costimulatory T-cell engagement by the 4-1BB/HER2 bispecific antibody-anticalin fusion PRS-343. *Clin. Cancer Res.* **2019**, *25*, 5878−5889.

(9) Ho, S. K.; Xu, Z.; Thakur, A.; Fox, M.; Tan, S. S.; DiGiammarino, E.; Zhou, L.; Sho, M.; Cairns, B.; Zhao, V.; Xiong, M.; Samayoa, J.; Forsyth, C. M.; Powers, D. B.; Chao, D. T.; Hollenbaugh, D.; Alvarez, H. M.; Akamatsu, Y. Epitope and Fc-mediated crosslinking, but not high affinity, are critical for antitumor activity of CD137 agonist antibody with reduced liver toxicity. *Mol. Cancer Ther.* **2020**, *19*, 1040−1051.

(10) Mikkelsen, K.; Harwood, S. L.; Compte, M.; Merino, N.; Molgaard, K.; Lykkemark, S.; Alvarez-Mendez, A.; Blanco, F. J.; Alvarez-Vallina, L. Carcinoembryonic antigen (CEA)-specific 4-1BB-costimulation induced by CEA-targeted 4-1BB-agonistic trimerbodies. *Front. Immunol.* **2019**, *10*, No. 01791.

(11) Stumpp, M. T.; Dawson, K. M.; Binz, H. K. Beyond antibodies: The DARPin drug platform. *BioDrugs* **2020**, *34*, 423−433.

(12) Cohen, S.; Chung, S.; Spiess, C.; Lundin, V.; Stefanich, E.; Laing, S. T.; Clark, V.; Brumm, J.; Zhou, Y.; Huang, C.; Guerrero, J.; Myneni, S.; Yadav, R.; Siradze, K.; Peng, K. An integrated approach for characterizing immunogenic responses toward a bispecific antibody. *mAbs* **2021**, *13*, No. 1944017.

(13) Schmidt, M. M.; Wittrup, K. D. A modeling analysis of the effects of molecular size and binding affinity on tumor targeting. *Mol. Cancer Ther.* **2009**, *8*, 2861−2871.

(14) Clement, K.; van den Akker, E.; Argente, J.; Bahm, A.; Chung, W. K.; Connors, H.; De Waele, K.; Farooqi, I. S.; Gonneau-Lejeune, J.; Gordon, G.; Kohlsdorf, K.; Poitou, C.; Puder, L.; Swain, J.; Stewart, M.; Yuan, G.; Wabitsch, M.; Kuhnen, P.; Setmelanotide, P.; L, P. T. Investigators, efficacy and safety of setmelanotide, an MC4R agonist, in individuals with severe obesity due to LEPR or POMC deficiency: single-arm, open-label, multicentre, phase 3 trials. *Lancet Diabetes Endocrinol.* **2020**, *8*, 960−970.

(15) Liao, D. S.; Grossi, F. V.; El Mehdi, D.; Gerber, M. R.; Brown, D. M.; Heier, J. S.; Wykoff, C. C.; Singerman, L. J.; Abraham, P.; Grassmann, F.; Nuernberg, P.; Weber, B. H. F.; Deschatelets, P.; Kim, R. Y.; Chung, C. Y.; Ribeiro, R. M.; Hamdani, M.; Rosenfeld, P. J.; Boyer, D. S.; Slakter, J. S.; Francois, C. G. Complement C3 inhibitor pegcetacoplan for geographic atrophy secondary to age-related macular degeneration: A randomized phase 2 trial. *Ophthalmology* **2020**, *127*, 186−195.

(16) Howard, J. F., Jr.; Nowak, R. J.; Wolfe, G. I.; Freimer, M. L.; Vu, T. H.; Hinton, J. L.; Benatar, M.; Duda, P. W.; MacDougall, J. E.; Farzaneh-Far, R.; Kaminski, H. J.; Zilucoplan MG Study Group. Clinical effects of the self-administered subcutaneous complement inhibitor zilucoplan in patients with moderate to severe generalized myasthenia gravis: results of a phase 2 randomized, double-blind, placebo-controlled, multicenter clinical trial. *JAMA Neurol.* **2020**, *77*, 582−592.

(17) Teufel, D. P.; Bennett, G.; Harrison, H.; van Rietschoten, K.; Pavan, S.; Stace, C.; Le Floch, F.; Van Bergen, T.; Vermassen, E.; Barbeaux, P.; Hu, T. T.; Feyen, J. H. M.; Vanhove, M. Stable and long-lasting, novel bicyclic peptide plasma kallikrein inhibitors for the treatment of diabetic macular edema. *J. Med. Chem.* **2018**, *61*, 2823−2836.

(18) Bennett, G.; Brown, A.; Mudd, G.; Huxley, P.; Van Rietschoten, K.; Pavan, S.; Chen, L.; Watcham, S.; Lahdenranta, J.; Keen, N. MMAE delivery using the bicycle toxin conjugate BT5528. *Mol. Cancer Ther.* **2020**, *19*, 1385−1394.

(19) Mayes, P. A.; Hance, K. W.; Hoos, A. The promise and challenges of immune agonist antibody development in cancer. *Nat. Rev. Drug Discovery* **2018**, *17*, 509−527.

(20) Wang, R.; Gao, C.; Raymond, M.; Dito, G.; Kabbabe, D.; Shao, X.; Hilt, E.; Sun, Y.; Pak, I.; Gutierrez, M.; Melero, I.; Spreafico, A.; Carvajal, R. D.; Ong, M.; Olszanski, A. J.; Milburn, C.; Thudium, K.; Yang, Z.; Feng, Y.; Fracasso, P. M.; Korman, A. J.; Aanur, P.; Huang, S. A.; Quigley, M. An Integrative approach to inform optimal administration of OX40 agonist antibodies in patients with advanced solid tumors. *Clin. Cancer Res.* **2019**, *25*, 6709−6720.

(21) Upadhyaya, P.; Lahdenranta, J.; Hurov, K.; Battula, S.; Dods, R.; Haines, E.; Kleyman, M.; Kristensson, J.; Kublin, J.; Lani, R.; Ma, J.; Mudd, G.; Repash, E.; Van Rietschoten, K.; Stephen, T.; You, F.; Harrison, H.; Chen, L.; McDonnell, K.; Brandish, P.; Keen, N. Anticancer immunity induced by a synthetic tumor-targeted CD137 agonist. *J. Immunother. Cancer* **2021**, *9*, No. e001762.

(22) Deng, H.; Shi, H.; Chen, L.; Zhou, Y.; Jiang, J. Over-expression of nectin-4 promotes progression of esophageal cancer and correlates with poor prognosis of the patients. *Cancer Cell Int.* **2019**, *19*, No. 106.

(23) Challita-Eid, P. M.; Satpayev, D.; Yang, P.; An, Z.; Morrison, K.; Shostak, Y.; Raitano, A.; Nadell, R.; Liu, W.; Lortie, D. R.; Capo, L.; Verlinsky, A.; Leavitt, M.; Malik, F.; Avina, H.; Guevara, C. I.; Dinh, N.; Karki, S.; Anand, B. S.; Pereira, D. S.; Joseph, I. B.; Donate, F.; Morrison, K.; Stover, D. R. Enfortumab vedotin antibody-drug conjugate targeting nectin-4 is a highly potent therapeutic agent in multiple preclinical cancer models. *Cancer Res.* **2016**, *76*, 3003−3013.

(24) Hurov, K.; Lahdenranta, J.; Upadhyaya, P.; Haines, E.; Cohen, H.; Repash, E.; Kanakia, D.; Ma, J.; Kristensson, J.; You, F.; Campbell, C.; Witty, D.; Kelly, M.; Blakemore, S.; Jeffrey, P.; McDonnell, K.; Brandish, P.; Keen, N. BT7480, a novel fully synthetic bicycle tumor-targeted immune cell agonist (Bicycle TICA) induces tumor localized CD137 agonism. *J. Immunother. Cancer* **2021**, *9*, No. e002883.

(25) Douglass, E. F., Jr.; Miller, C. J.; Sparer, G.; Shapiro, H.; Spiegel, D. A. A comprehensive mathematical model for three-body binding equilibria. *J. Am. Chem. Soc.* **2013**, *135*, 6092−6099.

(26) Bartkowiak, T.; Curran, M. A. 4-1BB agonists: multi-potent potentiators of tumor immunity. *Front. Oncol.* **2015**, *5*, No. 117.

(27) Chin, S. M.; Kimberlin, C. R.; Roe-Zurz, Z.; Zhang, P.; Xu, A.; Liao-Chan, S.; Sen, D.; Nager, A. R.; Oakdale, N. S.; Brown, C.; Wang, F.; Yang, Y.; Lindquist, K.; Yeung, Y. A.; Salek-Ardakani, S.; Chaparro-Riggers, J. Structure of the 4-1BB/4-1BBL complex and distinct binding and functional properties of utomilumab and urelumab. *Nat. Commun.* **2018**, *9*, No. 4679.

(28) Klinghoffer, R. A.; Bahrami, S. B.; Hatton, B. A.; Frazier, J. P.; Moreno-Gonzalez, A.; Strand, A. D.; Kerwin, W. S.; Casalini, J. R.; Thirstrup, D. J.; You, S.; Morris, S. M.; Watts, K. L.; Veiseh, M.; Grenley, M. O.; Tretyak, I.; Dey, J.; Carleton, M.; Beirne, E.; Pedro, K. D.; Ditzler, S. H.; Girard, E. J.; Deckwerth, T. L.; Bertout, J. A.; Meleo, K. A.; Filvaroff, E. H.; Chopra, R.; Press, O. W.; Olson, J. M. A technology platform to assess multiple cancer agents simultaneously within a patient's tumor. *Sci. Transl. Med.* **2015**, *7*, No. 284ra258.

(29) Butreddy, A.; Gaddam, R. P.; Kommineni, N.; Dudhipala, N.; Voshavar, C. PLGA/PLA-based long-acting injectable depot microspheres in clinical use: production and characterization overview for protein/peptide delivery. *Int. J. Mol. Sci.* **2021**, *22*, 8884.

(30) Bech, E. M.; Pedersen, S. L.; Jensen, K. J. Chemical strategies for half-life extension of biopharmaceuticals: lipidation and its alternatives. *ACS Med. Chem. Lett.* **2018**, *9*, 577−580.

(31) Chae, S. Y.; Jin, C. H.; Shin, H. J.; Youn, Y. S.; Lee, S.; Lee, K. C. Preparation, characterization, and application of biotinylated and biotin-PEGylated glucagon-like peptide-1 analogues for enhanced oral delivery. *Bioconjugate Chem.* **2008**, *19*, 334−341.

(32) Pollaro, L.; Raghunathan, S.; Morales-Sanfrutos, J.; Angelini, A.; Kontos, S.; Heinis, C. Bicyclic peptides conjugated to an albumin-binding tag diffuse efficiently into solid tumors. *Mol. Cancer Ther.* **2015**, *14*, 151−161.

(33) Bartkowiak, T.; Jaiswal, A. R.; Ager, C. R.; Chin, R.; Chen, C. H.; Budhani, P.; Ai, M.; Reilley, M. J.; Sebastian, M. M.; Hong, D. S.; Curran, M. A. Activation of 4-1BB on liver myeloid cells triggers hepatitis via an interleukin-27-dependent pathway. *Clin. Cancer Res.* **2018**, *24*, 1138−1151.

(34) Bajaj, G.; Nazari, F.; Presler, M.; Thalhauser, C.; Forssmann, U.; Jure-Kunkel, M.; Muik, A.; Lagkadinou, E.; Tureci, Ö.; Sahin, U.; Ahmadi, T.; Gupta, M. Dose selection for DuoBody-PD-L1×4-1BB (GEN1046) using a semimechanistic pharmacokinetics/ pharmacodynamics model that leverages preclinical and clinical data. *J. Immunother. Cancer* **2021**, *9*, No. A821.

(35) Barré, J.; Chamouard, J. M.; Houin, G.; Tillement, J. P. Equilibrium dialysis, ultrafiltration, and ultracentrifugation compared for determining the plasma-protein-binding characteristics of valproic acid. *Clin. Chem.* **1985**, *31*, 60−64.